Supporting Information

Electronic structure modification and N-doped carbon shell nanoarchitectonics of Ni_3FeN@NC for overall water splitting performance evaluation

Dong In Jeong[a‡], Hyung Wook Choi[b‡], Seongwon Woo[a], Jung Hyeon Yoo[a], Donghyeon Kang[a], SeongMin Kim[a], Byungkwon Lim[a], Jung Ho Kim[e], Sang-Woo Kim[ab], Bong Kyun Kang[cd] and Dae Ho Yoon[ab*]*

[a]School of Advanced Materials Science and Engineering, Sungkyunkwan University, Suwon 440-746, Republic of Korea

[b]SKKU Advanced Institute of Nanotechnology (SAINT), Sungkyunkwan University, Suwon 16419, Republic of Korea

[c]Department of Electronic Materials, Devices, and Equipment Engineering, Soonchunhyang University,22, Soonchunhyang-ro, Asan City, Chungnam, 31538, Republic of Korea

[d]Department of Display Materials Engineering, Soonchunhyang University, 22, Soonchunhyang-ro, Asan City, Chungnam, 31538, Republic of Korea

[e]Australian Institute for Innovative Materials (AIIM), University of Wollongong, Squires Way, North Wollongong, NSW 2500, Australia

E-mail address: kangbk84@sch.ac.kr (B.K. Kang), dhyoon@skku.edu (D.H. Yoon)

KEYWORDS: Transition metal nitride, N-doped carbon shell, Overall Water Splitting Catalysts, Density Functional Theory, Oxygen evolution reaction, Hydrogen evolution reaction.

Computational details

To investigate the electronic structure of material, we used CASTEP code, as implemented in Material Studio.[1] A general procedure for DFT setting is described elsewhere.[2] The electron-ion interactions by treating valence electrons of atom were demonstrated by the on-the-fly-generation (OTFG) ultrasoft pseudopotential, and the generalized gradient approximation (GGA) with Perdew, Burke and Ernzerhof (PBE) for exchange-correlation functional with BFGS algorithm was used for the structure optimization. Since Ni and Fe are transition metals with possessing magnetic moments, spin optimization was also carried out during cell optimization of bulk Ni_3Fe and Ni_3FeN. The cleavage and interface were investigated using a slab and contact model, which has more than 15 Å vacuum region for neglecting spurious interaction between the neighboring unit cells. Convergence acting forces on atoms were 0.03 eV $Å^{-1}$, k-spacing of ~ 0.04 $Å^{-1}$ is used for density of states (DOS) and band structure calculations in structure optimization. For a contact model with carbon shells on top of the slabs, long-range energy correction is analyzed using TS scheme (semiempirical dispersion correction) to describe molecular van der Waals interactions.[3]

Besides the DOS calculation of Ni_3FeN and Ni_3Fe, simulations of Gibbs energy diagram in OER, HER and charge distribution according to the catalytic reaction were performed on the (111) plane. The change in Gibbs free energy shown in the energy diagram was obtained through the bonding energy between the Fe element on the (111) plane of Ni_3FeN and Ni_3Fe

and *OH, *OOH, *O for each step. Additionally, μ_*^o is the Gibbs free energy ($H - T\Delta S$) of a pure transition metal compound that does not contain by-products generated during the catalyst intermediate process between Ni_3FeN and Ni_3Fe materials.[4] We confirmed how the path of four-electrons ($4e^-$) occurs in an alkaline environment during the OER reaction in the equation : [5]

For step 1,

$$\Delta G_1^o = \mu_{*OH}^o + \mu_{e^-}^o - \mu_{OH^-}^o - \mu_*^o$$

$$= \mu_{*OH}^o + \mu_{e^-}^o - (\mu_{H_2O}^o - \mu_{H^+}^o) - \mu_*^o$$

$$= \mu_{*OH}^o - \mu_{H_2O}^o + \frac{1}{2}\mu_{H_2}^o - \mu_*^o$$

$$= E_{total}(*OH) - E_{total}(H_2O) + \frac{1}{2}E_{total}(H_2) - E_{tatal}(*)$$

$$= \left[H_{total}(*OH) - H_{total}(H_2O) + \frac{1}{2}H_{total}(H_2) - H_{total}(*)\right] - T\left[S_{to}\right.$$

For step 2,

$$\Delta G_2^o = \mu_{*O}^o + \mu_{H^+}^o + \mu_{e^-}^o - \mu_{*OH}^o$$

$$= \mu_{*O}^o + \frac{1}{2}\mu_{H_2}^o - \mu_{*OH}^o$$

$$= E_{total}(*O) + \frac{1}{2}E_{total}(H_2) - E_{tatal}(*OH)$$

$$= \left[H_{total}(*O) + \frac{1}{2}H_{total}(H_2) - H_{total}(*OH)\right] - T\left[S_{total}(*O) + \frac{1}{2}\right.$$

For step 3,

$$\Delta G_3^o = \mu_{*OOH}^o + \mu_{H^+}^o + \mu_{e^-}^o - \mu_{*O}^o - \mu_{H_2O}^o$$

$$\Delta G_3^o = \mu_{*OOH}^o + \mu_{H^+}^o + \mu_{e^-}^o - \mu_{*O}^o - \mu_{H_2O}^o$$

$$= \mu_{*OOH}^o + \frac{1}{2}\mu_{H_2}^o - \mu_{*O}^o - \mu_{H_2O}^o$$

$$= E_{total}(*OOH) + \frac{1}{2}E_{total}(H_2) - E_{total}(*O) - E_{total}(H_2O)$$

$$= \left[H_{total}(*OOH) + \frac{1}{2}H_{total}(H_2) - H_{total}(*O) - H_{total}(H_2O)\right] - T\left[\right.$$

For step 4,

$$\Delta G_4^o = \mu_*^o + \mu_{O_2}^o + \mu_{H^+}^o + \mu_{e^-}^o - \mu_{*OOH}^o$$

$$= \mu_*^o + \mu_{O_2}^o + \frac{1}{2}\mu_{H_2}^o - \mu_{*OOH}^o$$

$$= E_{total}(*) + E_{total}(O_2) + \frac{1}{2}E_{total}(H_2) - E_{total}(*OOH)$$

$$= \left[H_{total}(*) + H_{total}(O_2) + \frac{1}{2}H_{total}(H_2) - H_{total}(*OOH)\right] - T\left[S_{to}\right.$$

μ_*^o is the DFT calculated total electronic energy for Ni_3FeN and Ni_3Fe atomic model structure, and for each μ_{*OH}^o, μ_{*O}^o, and μ_{*OOH}^o, it is the electronic energy of OH, O, and OOH attached to the Fe site on each (111) surface of the Ni_3FeN and Ni_3Fe model structure. Additionally, calculations for $\mu_{OH^-}^o$ in all steps are derived from $\mu_{H_2O}^o - \mu_{H^+}^o$ and $\frac{1}{2}\mu_{H_2}^o$ is derived from $\mu_{H^+}^o + \mu_{e^-}^o$ equations.[6]

HER

$$\Delta G_1^o = \mu_{*H}^o - \mu_{e^-}^o - \mu_{H^+}^o - \mu_*^o$$

$$= \mu_{*H}^o + \frac{1}{2}\mu_{H_2}^o - \mu_*^o$$

$$= E_{total}(*H) + \frac{1}{2}E_{total}(H_2) - E_{tatal}(*)$$

$$= \left[H_{total}(*H) + \frac{1}{2}H_{total}(H_2) - H_{tatal}(*)\right] - T\left[S_{total}(*H) + \frac{1}{2}S_{total}(H_2) - S_{tatal}(*)\right]$$

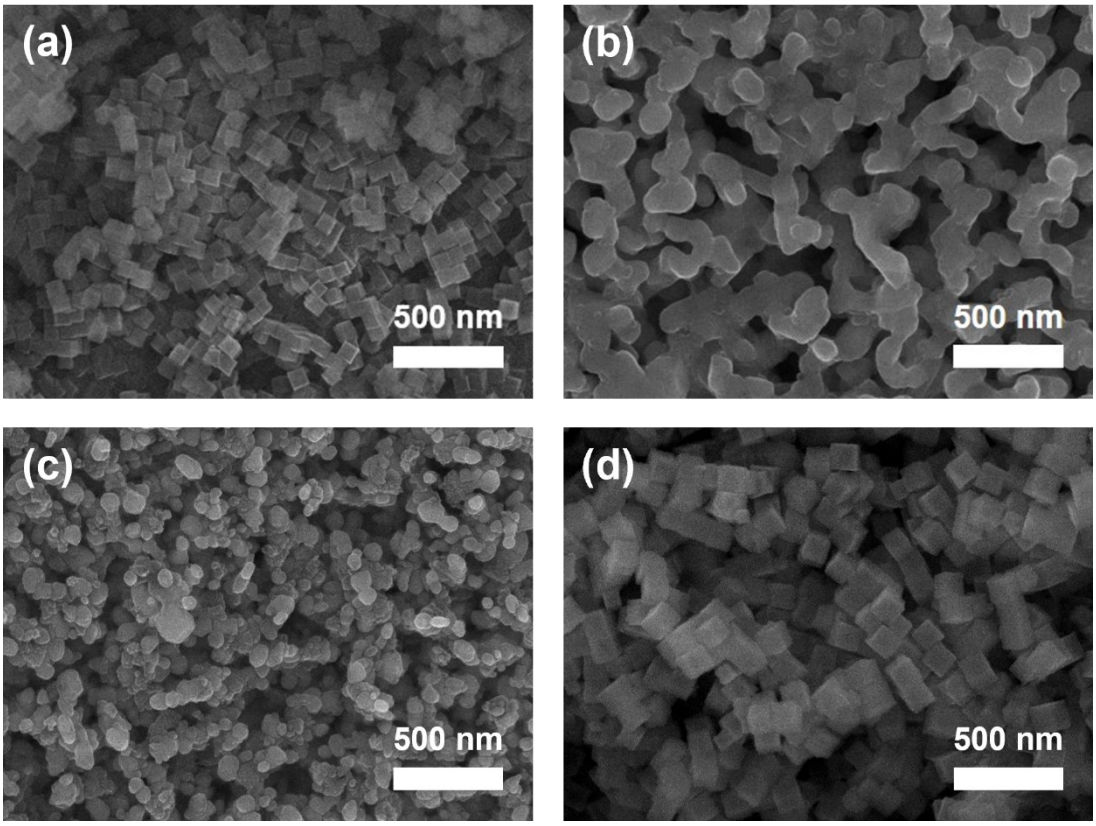

Fig. S1 SEM image of (a) $Ni_3[Ni_{0.375}Fe_{0.625}(CN)_6]_2$ PBA precursor, (b) Ni_3FeN@NC, (c) Ni_3Fe@NC, and $NiO/NiFe_2O_4$.

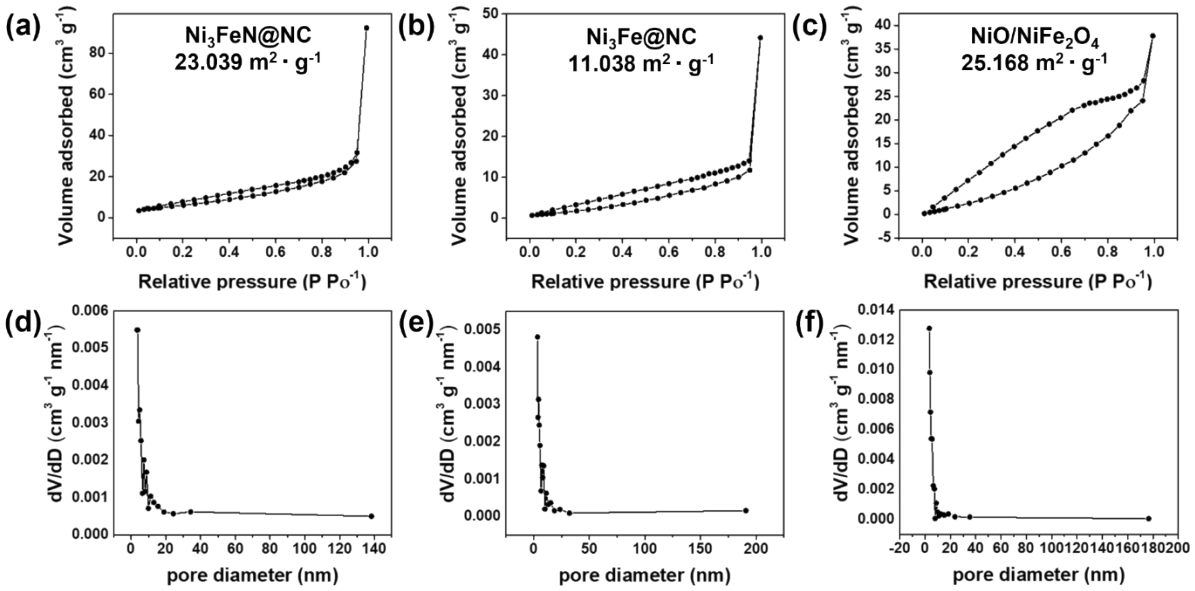

Fig. S2 Nitrogen adsorption-desorption isotherms and pore size distribution of (a, d) Ni_3FeN@NC, (b, e) Ni_3Fe@NC, and (c, f) $NiO/NiFe_2O_4$.

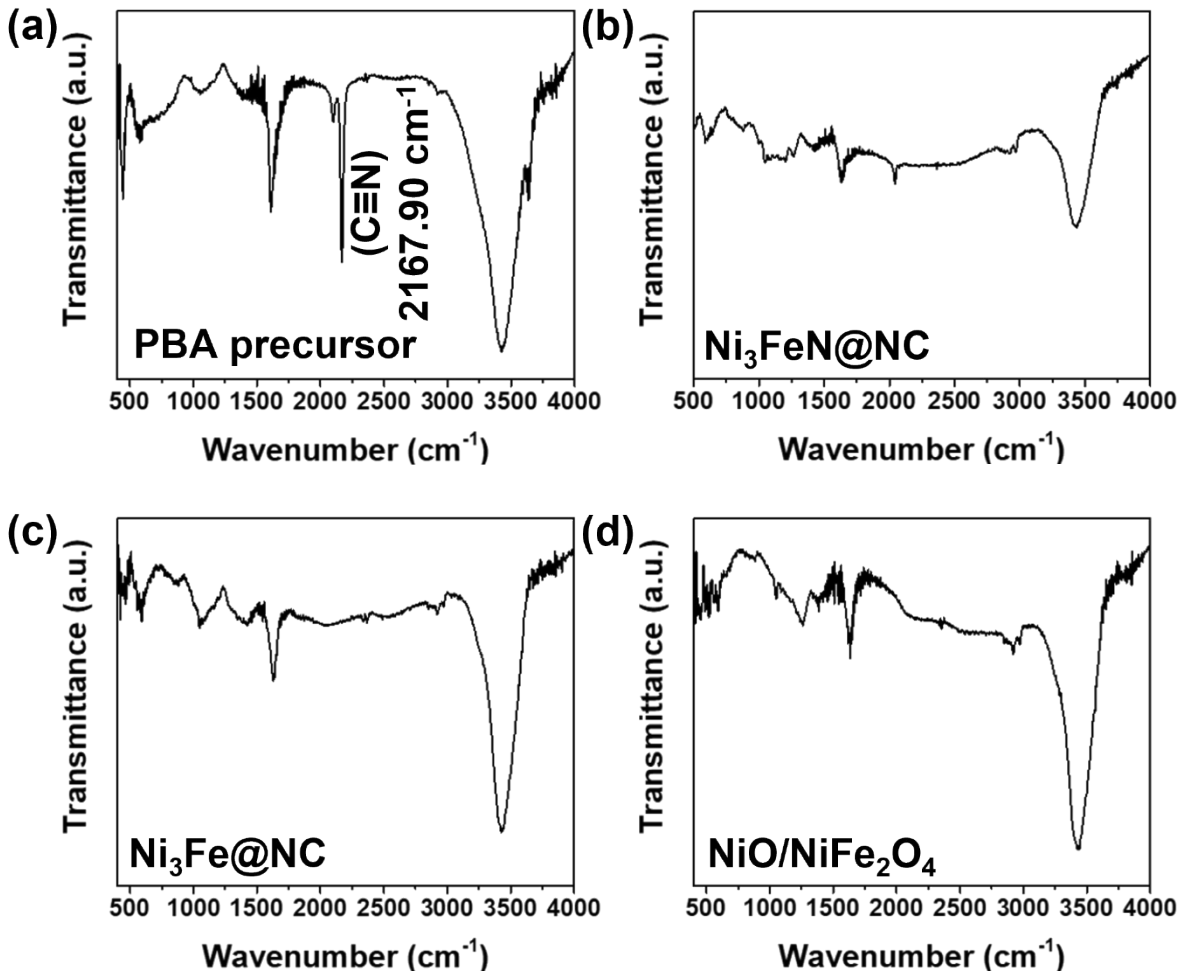

Fig. S3 FT-IR characterization of (a) $Ni_3[Ni_{0.375}Fe_{0.625}(CN)_6]_2$ PBA precursor, (b) Ni_3FeN@NC, (c) Ni_3Fe@NC, and NiO/$NiFe_2O_4$.

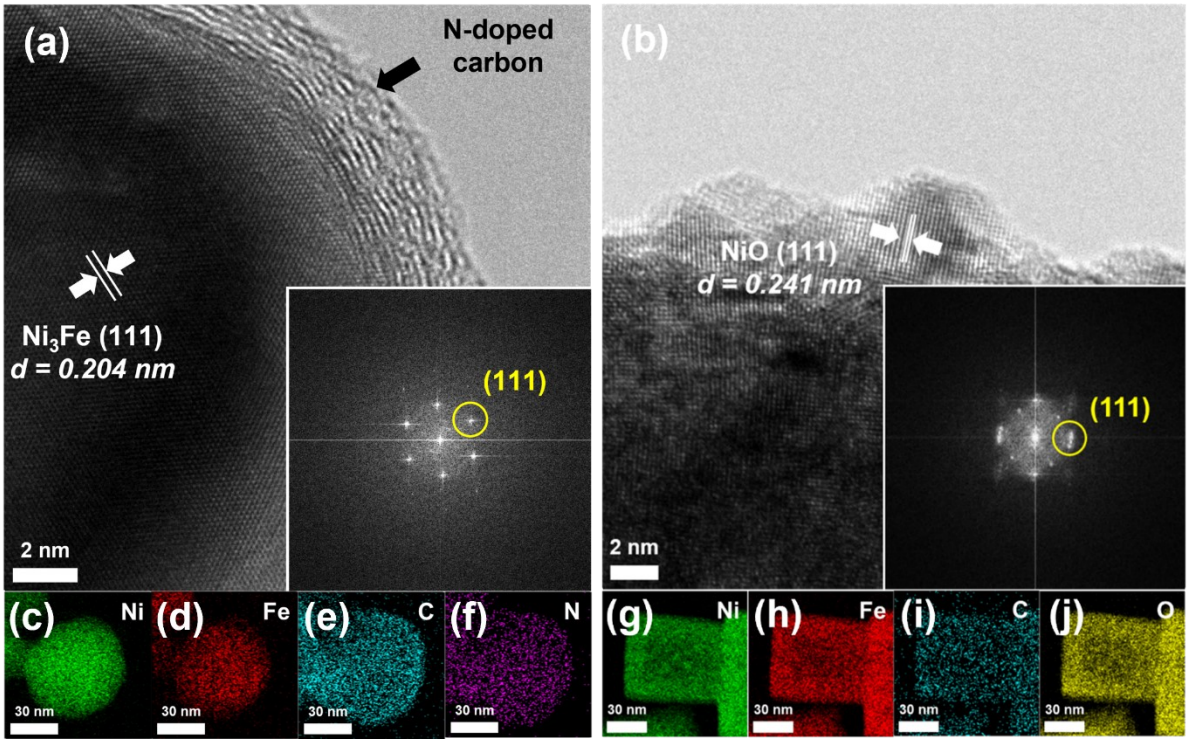

Fig. S4 (a, b) HRTEM (the inset shows the corresponding SAED pattern) image of Ni_3Fe@NC, and NiO/$NiFe_2O_4$. Elemental mapping of (c) Ni, (d) Fe, (e) C, (f) N on Ni_3Fe@NC and (g) Ni, (h) Fe, (i) C, (j) O on NiO/$NiFe_2O_4$.

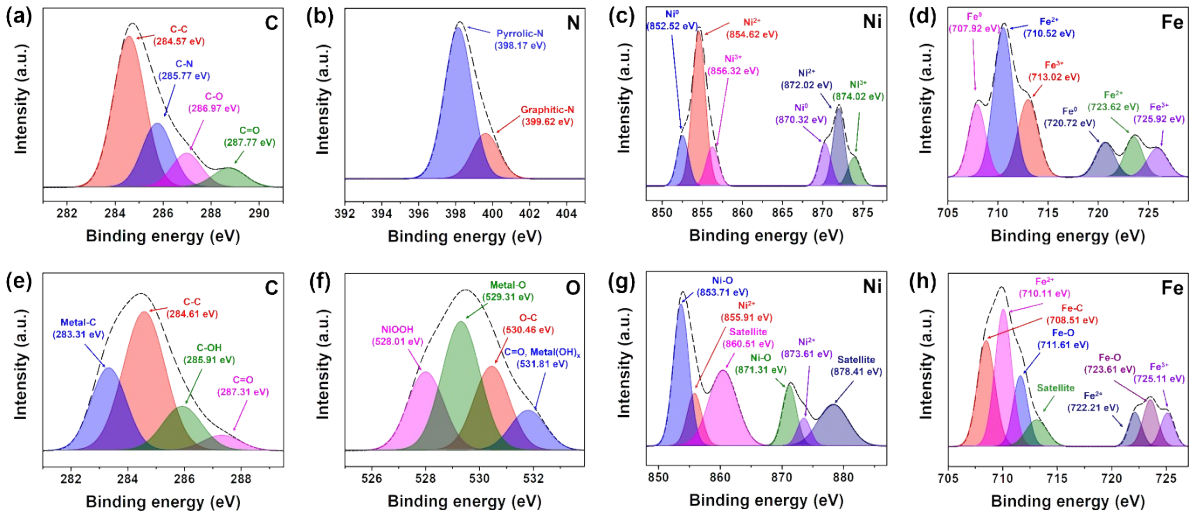

Fig. S5 The high-resolution XPS of (a) C, (b) N, (c) Ni (d) Fe spectrum on the surface of Ni_3Fe@NC and (e) C, (f) O, (g) Ni, and (h) Fe spectrum on the surface of $NiO/NiFe_2O_4$.

Catalyst	OER overpotential (η) at 10 mA · cm^{-2} (mV)	HER overpotential (η) at 10 mA · cm^{-2} (mV)	Electrode materials	Electrolyte	Reference
Ni_3FeN@NC	246	181	Carbon paper	1.0 M KOH	This work
Ni_3FeN	241	238	Carbon cloth	1.0 M KOH	7
Co-Ni_3N	307	194	Carbon cloth	1.0 M KOH	8
Ni_3FeN-NPs	280	158	Nickel foam	1.0 M KOH	9
Ni_3FeN-Bulk	310	208	Nickel foam	1.0 M KOH	9
Co@N-C	400	210	Carbon paper	1.0 M KOH	10
NiFeOP	310	209	Carbon paper	1.0 M KOH	11
NiFe@OCC	281	256	Carbon cloth	1.0 M KOH	12
$Ni_{1.5}Fe_{0.5}P$/CF	264	282	Glassy carbon	1.0 M KOH	13
FeCoNiP@NC	266	187	Graphite plate	1.0 M KOH	14
Fe-Ni@NC-CNT	274	202	Nickel foam	1.0 M KOH	15
$Ni_{0.95}Fe_{0.05}$LDH	330	200	Carbon paper	1.0 M KOH	16
Co-Mo_2C @NCNT	377	186	Glassy carbon	1.0 M KOH	17
CoP-NC@NFP	270	162	Nickel foam	1.0 M KOH	18
Co_4Ni_1S/CC	296	192	Carbon cloth	1.0 M KOH	19
NiCoFeP/C	270	149	Carbon paper	1.0 M KOH	20
Ni-Co-P	270	107	Nickel foam	1.0 M KOH	21
Ni-M@C-130	244	123	Nickel foam	1.0 M KOH	22

Table S1 Comparison of electrocatalytic performances of Ni_3FeN@NC with other transition metal, carbon based electrocatalysts for OER, HER in alkaline media at 10 mA · cm^{-2} (mV).

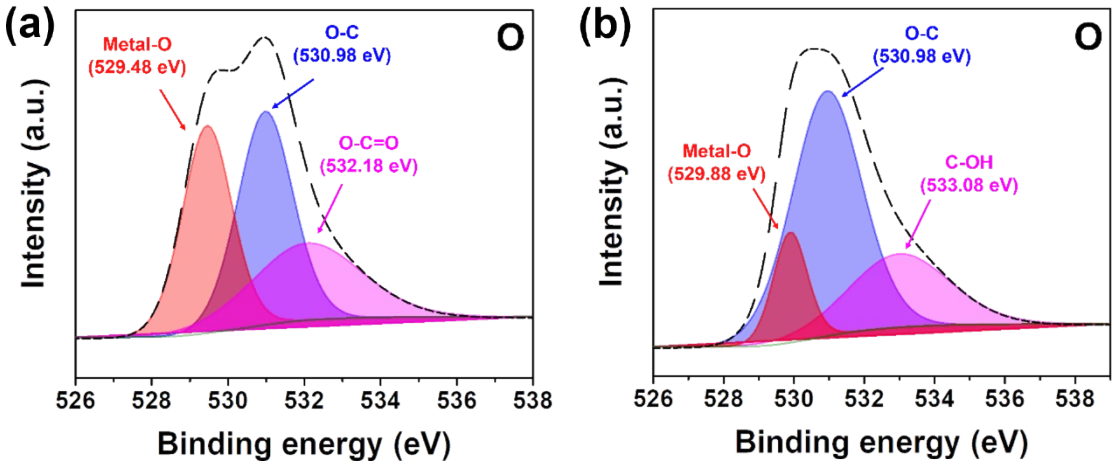

Fig. S6 The high-resolution XPS of before electrochemical analysis O spectrum on the surface of (a) Ni_3FeN@NC, and (b) Ni_3Fe@NC.

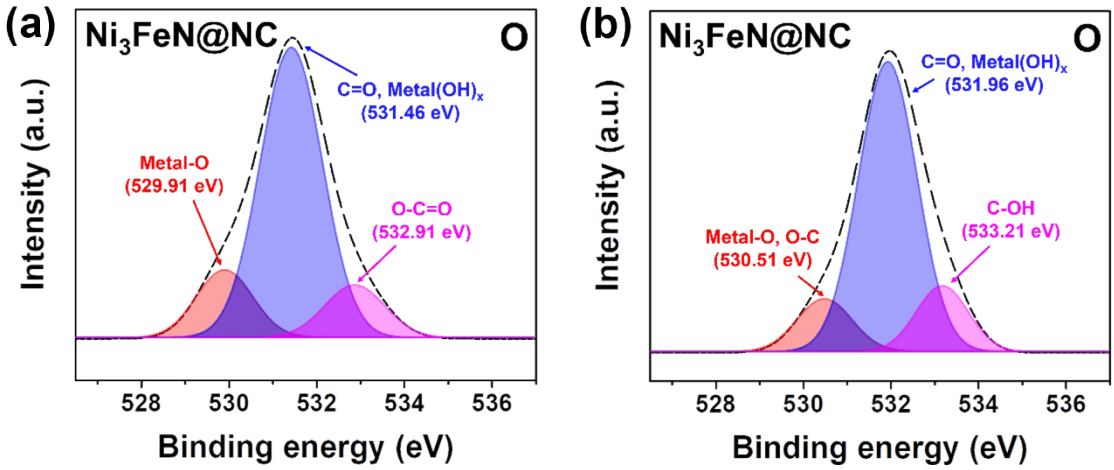

Fig. S7 Atter step stability (a) OER and (b) HER of Ni_3FeN@NC high-resolution XPS of O spectrum on the surface.

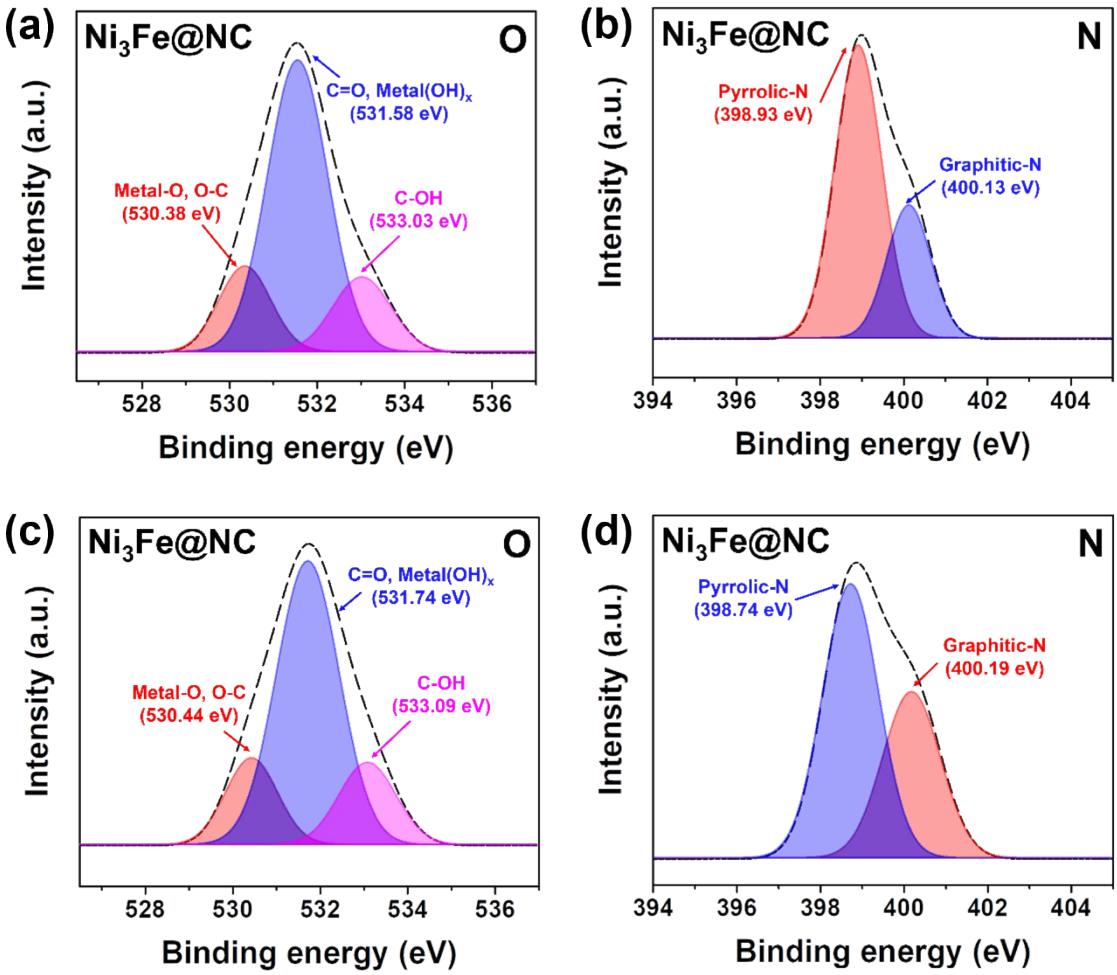

Fig. S8 Atter step stability (a and b) OER and (c and d) HER of Ni_3Fe@NC high-resolution XPS of O and N spectrum on the surface.

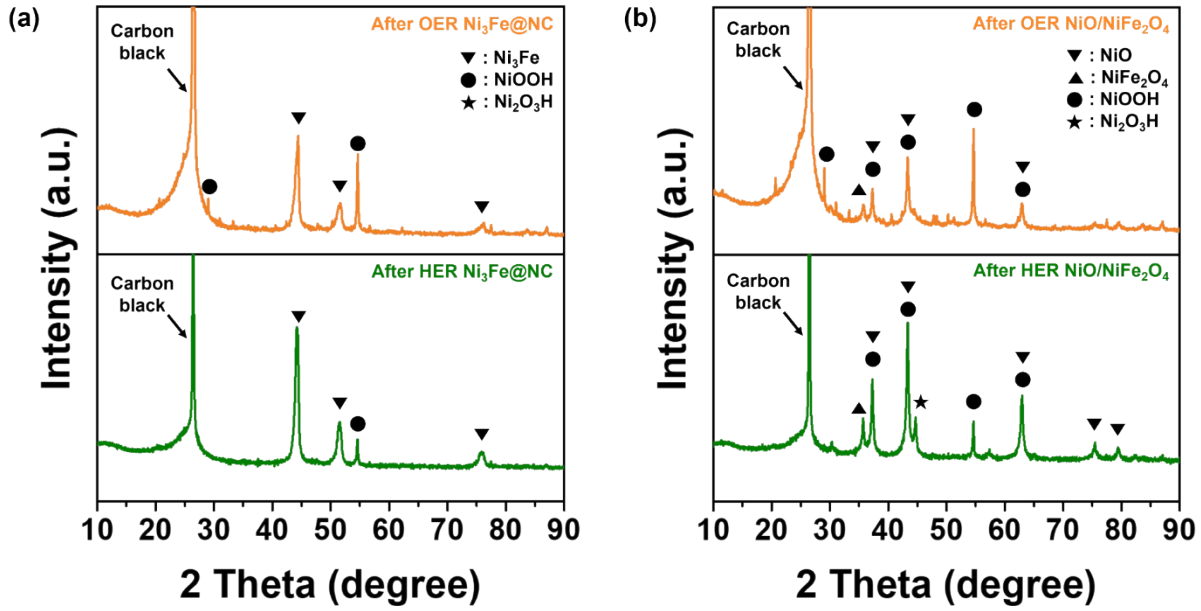

Fig. S9 XRD patterns of after step stability (a) Ni_3Fe@NC, and (b) $NiO/NiFe_2O_4$ on carbon paper.

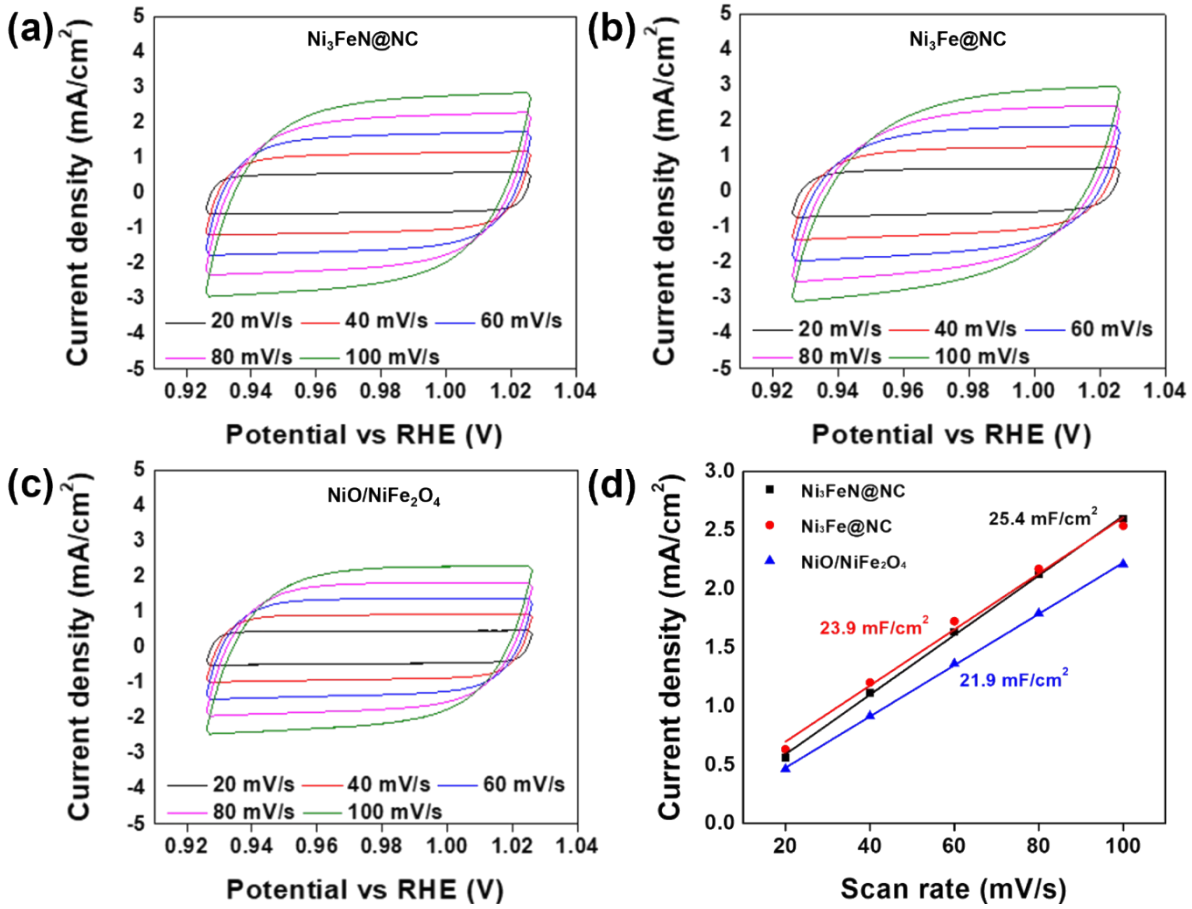

Fig. S10 CVs scanned at different rates in the fixed potential ranges vs RHE for (a) Ni_3FeN@NC, (b) Ni_3Fe@NC, and (c) NiO/$NiFe_2O_4$. (d) ECSA of Ni_3FeN@NC, Ni_3Fe@NC, and NiO/$NiFe_2O_4$.

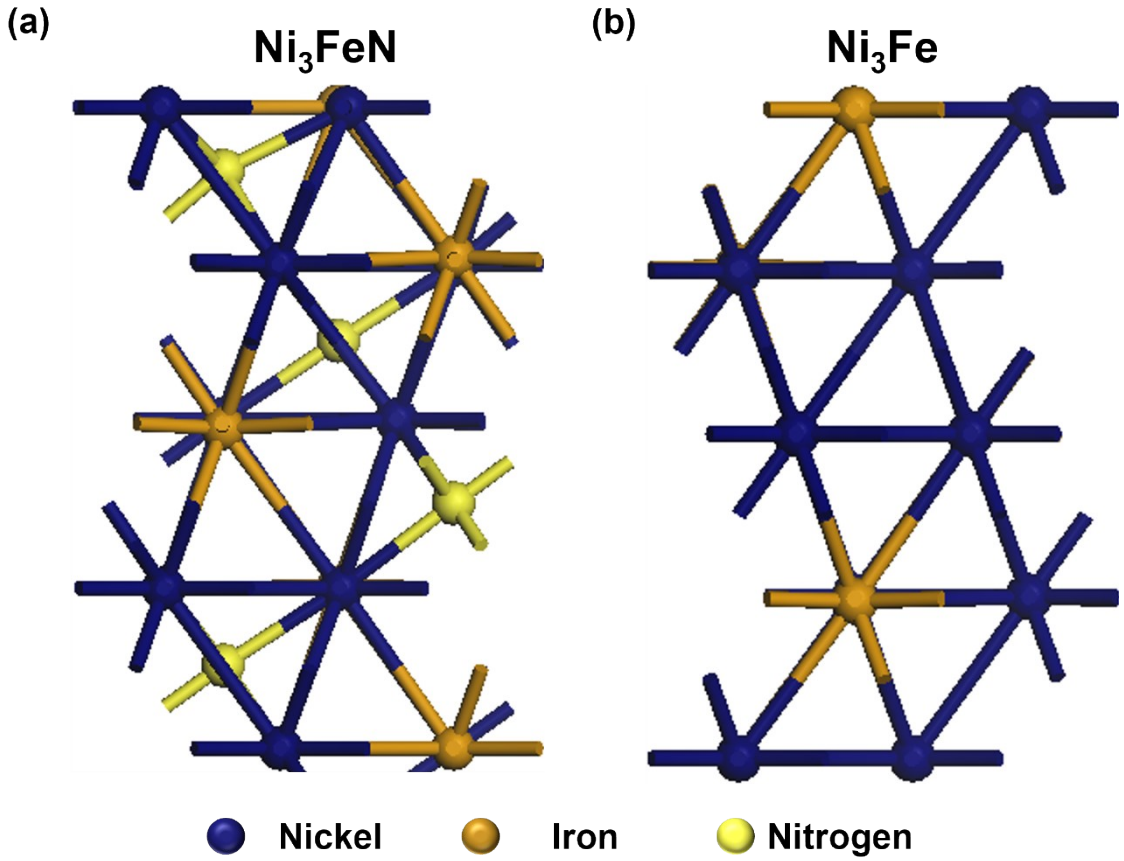

Fig. S11 Optimized atomic structures of (a) Ni_3FeN and (b) Ni_3Fe with different atomic color were calculated by DFT.

Reference

1. S.J. Clark, M.D. Segall, C.J. Pickard, P.J. Hasnip, M.I.J. Probert, K. Refson, M. C. Payne, *Z. Kristallogr, Cryst. Mater.,* **220**, 567–570 (2005).
2. D. Kang, H. Y. Lee, J.-H. Hwang, S. Jeon, D. Kim, S.M. Kim, S.-W. Kim, *Nano Energy,* **100**, 107531 (2022).
3. A. Tkatchenko and M. Scheffler, *Phy. Rev. Lett.,* **102**, 073005 (2009).
4. X. Jia, Y. Zhao, G. Chen, L. Shang, R. Shi, X. Kang, G. I. Waterhouse, L. Z. Wu, C. H. Tung and T. Zhang, *Adv. Energy Mater.*, 2016, **6**, 1502585.
5. C. H. Lee, B. Jun and S. U. Lee, *ACS Sustain. Chem. Eng.*, 2018, **6**, 4973-4980.
6. Z. Liang, X. Zhong, T. Li, M. Chen and G. Feng, *ChemElectroChem*, 2019, **6**, 260-267.
7. X. Jia, Y. Zhao, G. Chen, L. Shang, R. Shi, X. Kang, G. I. N. Waterhouse, L.-Z. Wu, C.-H. Tung and T. Zhang, *Adv. Energy Mater.*, 2016, **6**.
8. Q. Chen, R. Wang, M. Yu, Y. Zeng, F. Lu, X. Kuang and X. Lu, *Electrochim. Acta*, 2017, **247**, 666-673.
9. C. Zhu, A. L. Wang, W. Xiao, D. Chao, X. Zhang, N. H. Tiep, S. Chen, J. Kang, X. Wang, J. Ding, J. Wang, H. Zhang and H. J. Fan, *Adv Mater*, 2018, **30**, e1705516.
10. J. Wang, D. Gao, G. Wang, S. Miao, H. Wu, J. Li and X. Bao, *J. Mater. Chem. A*, 2014, **2**, 20067-20074.
11. J. Chen, Z. Guo, Y. Luo, M. Cai, Y. Gong, S. Sun, Z. Li and C.-J. Mao, *ACS Sustain. Chem. Eng.*, 2021, **9**, 9436-9443.
12. Y. Lv, A. Batool, Y. Wei, Q. Xin, R. Boddula, S. U. Jan, M. Z. Akram, L. Tian, B. Guo and J. R. Gong, *ChemElectroChem*, 2019, **6**, 2497-2502.
13. H. Huang, C. Yu, C. Zhao, X. Han, J. Yang, Z. Liu, S. Li, M. Zhang and J. Qiu, *Nano Energy*, 2017, **34**, 472-480.

14. J. Sun, S. Li, Q. Zhang and J. Guan, *Sustain. Energy Fuels*, 2020, **4**, 4531-4537.

15. X. Zhao, P. Pachfule, S. Li, J. R. J. Simke, J. Schmidt and A. Thomas, *Angew Chem Int Ed Engl*, 2018, **57**, 8921-8926.

16. X. Zhang, A. N. Marianov, Y. Jiang, C. Cazorla and D. Chu, *ACS Appl. Nano Mater.*, 2019, **3**, 887-895.

17. L. Ai, J. Su, M. Wang and J. Jiang, *ACS Sustain. Chem. Eng.*, 2018, **6**, 9912-9920.

18. E. Vijayakumar, S. Ramakrishnan, C. Sathiskumar, D. J. Yoo, J. Balamurugan, H. S. Noh, D. Kwon, Y. H. Kim and H. Lee, *Chem. Eng. J.*, 2022, **428**.

19. Y. Dong, Z. Fang, W. Yang, B. Tang and Q. Liu, *ACS Appl. Mater. Interfaces*, 2022, **14**, 10277-10287.

20. X. Wei, Y. Zhang, H. He, L. Peng, S. Xiao, S. Yao and P. Xiao, *ChemComm.*, 2019, **55**, 10896-10899.

21. E. Hu, Y. Feng, J. Nai, D. Zhao, Y. Hu and X. W. Lou, *Energy Environ. Sci.*, 2018, **11**, 872-880.

22. K. Srinivas, Y. Chen, X. Wang, B. Wang, M. Karpuraranjith, W. Wang, Z. Su, W. Zhang and D. Yang, *ACS Sustain. Chem. Eng.*, 2021, **9**, 1920-1931.